2017 IEEE Workshop on Modeling and Control in Power Electronics

Design and Implementation of a Lightweight High-Voltage Power Converter for Electro-aerodynamic Propulsion

Yiou He
Dept. Of Electrical Engineering and Computer Science
Massachusetts Institute of Technology
Cambridge, MA, USA
yiouhe@mit.edu

Mark Woolston
Lincoln Laboratory
Massachusetts Institute of Technology
Lexington, MA, USA
Mark.Woolston@ll.mit.edu

David Perreault
Dept. Of Electrical Engineering and Computer Science
Massachusetts Institute of Technology
Cambridge, MA, USA
djperrea@mit.edu

***Abstract*—Recent studies in electro-aerodynamic (EAD) propulsion have stimulated the need for lightweight power converters providing outputs at tens of kilovolts and hundreds of watts [1] [2]. This paper demonstrates a design of a lightweight high-voltage converter operating from a 160 – 200 V dc input and providing dc output of up to 600 W at 40 kV. It operates at around 500 kHz and achieves a specific power of 1.2 kW/kg. This is considerably lighter than comparable industrial and academic designs at this power level. High voltage converters generally comprise an inverter, a step-up transformer and a rectifier, with the large needed voltage gain distributed among these stages. Several means of realizing these stages are compared in terms of weight. The weight of the converter is minimized by properly selecting and optimizing the design and the voltage gain of each stage within the constraints of device limitations and losses. A prototype circuit is developed based on this approach and used to drive an EAD-propulsion system for an unmanned aerial vehicle (UAV). In addition to addressing the power conversion needs for EAD, this research can potentially benefit the development of lightweight high-voltage converters in many other applications where weight and size are important.**

Keywords—high voltage converter, lightweight, cockroft-walton, Dickson, high voltage diodes, electro-aerodynamic, EAD

I. INTRODUCTION

Weight reduction is particularly important in aerospace applications, including for high-voltage power supplies used in these applications. For high-power designs (e.g., tens to hundreds-of-kilovolts multi-megawatt power converters for space propulsion), the achievable specific power (gravimetric power density) has reached as high as 10 kW/kg [3] [4] [5] [6]. Recent advances in SiC devices have also helped with miniaturization of tens of kV and several-to-tens-of-kilowatts power converters. At these voltage and power level, power densities of above 1 kW/kg have been achieved [7].

However, there has been less research in reducing the weight of converters in the hundreds-of-watts and tens-of-kilovolts range. As shown in Fig. 1, a review of commercial products and academic designs in this range reveals that the specific power is typically around 0.1 kW/kg. In commerical high voltage power supplies in these power and voltage range, the switching frequency typically lies around 100 kHz or lower, resulting in bulky magnetics and capacitors. There have been

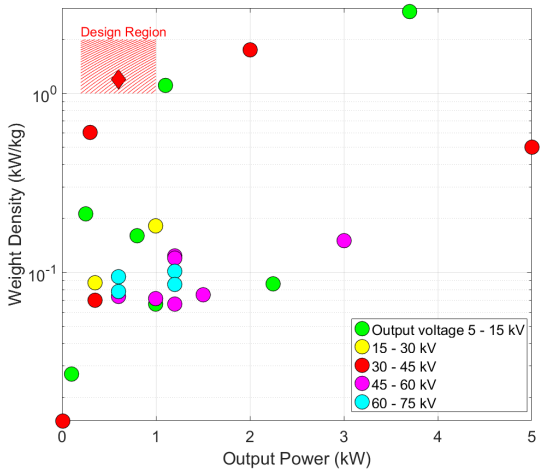

Fig. 1 Specific power of commercial and academic high-voltage converters at low to moderate power levels

research attempts to increase the switching frequency and specific power, but these have largely focused on cases of high input voltage (>= 400 V), low output voltage (<= 10 kV) and/or high power (> 2 kW) [7] [8] [9] [10] [11]. The detailed product list in this comparison is provided in the Appendix I.

One aspect of the differences in the specific power among high-voltage converter designs relates to the scaling of transformers. For low voltage levels (where insulation is not a limitation), the specific power (kW/kg) of transformers can be modeled to roughly scale with $(frequency)^{0.75}$ and $(power)^{0.25}$ [6] [12] [13] [14], indicating that specific power improves with higher power. Meanwhile, as transformer voltage increases, so do the challenges of insulation and inter-winding capacitance. These challenges bring new considerations in transformer design, such as sectioning the secondary and using thicker insulation, hurting specific power in ways not captured in [6] [12] [13] [14].

In many traditional applications at high-voltage and low power, such as X-ray machines, low-power electrostatic precipitators, etc., the weight of the power converter has not been a system-critical consideration. However, aerospace applications requiring low-power, high voltage conversion are emerging in which specific power is a major consideration. For example, electro-aerodynamic (EAD) propulsion has promise in UAV applications, owing to its high thrust-to-power ratio

and silent operation [1] [2]. An EAD-propulsion UAV has no moving parts; instead, the surrounding air is ionized and accelerated by a high potential gradient to generate an ionic wind. However, no UAV with EAD propulsion has ever flown, in large part due to the weight of the required power electronics. For a particular practical EAD UAV design under investigation by the authors and colleagues, the converter needs to convert from a battery voltage of 160 - 200 V dc to 40 kV dc and provide up to 600 W, with a specific power *above* 1 kW/kg.

This paper explores the design of a lightweight high-voltage power converter suitable for EAD propulsion system. A high voltage converter typically consists of three stages: a dc-ac inverter stage, an isolation/ transformation stage and an ac-dc rectifier stage. Passive components (inductors, transformers and capacitors), especially in the isolation and rectifier stage, contribute a major part of the weight. The paper firstly compares different approaches for voltage transformation and rectification in terms of the resulting weight. Furthermore, the overall weight of a converter based on the best identified approach is optimized by sweeping through combinations of voltage gain ratios with considerations of device limitations and losses. An optimized prototype converter rated at 40 kV and 600 W output is designed, constructed and tested, achieving a high specific power of 1.2 kW/kg, substantially higher than conventional designs in its power and voltage class.

Section II provides trade-offs among different rectifiers and isolation stages in terms of weight. Section III explains the optimization of the design. Section IV describes practical issues in building a lightweight high performance prototype, and presents experimental results from the prototype converter. Section V concludes the paper.

II. Topology Comparison and selection

High voltage dc-dc converters achieve large step-up voltage conversion using a combination of: (1) resonant and/or multi-level inverters; (2) large-turns-ratio transformers; (3) voltage multiplier rectifiers; and (4) parallel-input series-output structures [15]. In conventional designs, two major sources of the overall weight of the converter are the isolation stage (e.g. transformer core and windings) and rectifier stage (e.g. high voltage capacitors, diodes and potentially the required mechanical structures for support and cooling). Increasing the switching frequency of the converter can reduce the weight of both the transformer and the high voltage capacitors, however the feasibility of doing so is limited by the performance of available high-frequency high-voltage diodes.

This section first compares the weights of different rectifier topologies considering the characteristics of available high voltage capacitors and diodes. Second, to establish tradeoffs in reducing the weight of the isolation stage, it compares the weight of conventional cored transformers, resonant transformers and piezoelectric transformers. Based on the requirements of the EAD application, a specific topology and combination is chosen.

A. Components Selection

The weights and the efficiencies of high voltage rectifiers and multipliers in different topologies substantially depend on available high voltage capacitors and diodes. We have conducted a background study of some available high voltage capacitors and diodes, as shown in Appendix. 2.

1) High-Voltage Capacitor Selection

Mica, film and ceramic capacitors are commonly used in high voltage power converters. For the EAD application, the rated voltage, the capacitance and the weight of the capacitors are three main considerations. Whereas the ESR and the current carrying capability of the capacitors are less important because of the relatively small output current.

When the rated voltage is below several kV (~ 4 - 5 kV), there are SMT options in all three materials, ceramic capacitors with similar capacitance yields to slightly lower weight. There are limited options when the rated voltage goes above 8 kV. Mica and film capacitors are designed for high voltage high current applications, resulting in bigger package and heavier weights. Ceramic capacitors with leads offers medium capacitance (up to 1 nF) and relatively high rated voltage (up to 15 kV), and are much lighter options.

Two lightest options are using ceramic SMT capacitors rated below 5kV in series and parallel or using one single ceramic through-hole capacitor. The latter option are more compact, have less surface tracking issue and potentially eliminates the needs of using PCB. Among the investigated parts, Murata DHR series capacitors have the least weight in 10 – 15 kV range, thus they are used in the following calculations. At a given rated voltage, the weight of the capacitor is shown to be proportional to its capacitance, thus a linear relationship can be extrapolated for other capacitances at this voltage rating.

2) High-Voltage Diode Selection

High voltage diodes are a key limitation in building a high frequency high voltage converter at tens of kV and hundreds of W. Traditional Silicon high-voltage diodes (> 8kV) have longer recovery time comparing with their low-voltage counterparts, thus are typically used at frequencies below 200 kHz. Commercial high voltage SiC diodes are mostly rated under 3.3 kV. They have no recovery time but big parasitic capacitance since they are mainly designed for high current applications.

Some representative high voltage diodes are summarized in Appendix 2. Cree's C4D02120A, GeneSiC's GAP3SLT33-214 and VMI's VMI150FF3 are considered in later studies because of their small recovery time and relatively low parasitic capacitance. GAP05SLT80-220 could also be a good choice if at a more affordable price.

B. Comparison of voltage multiplier topologies

The typical topologies of the voltage multipliers (VM) used in high voltage converters include half-wave (H-W) and full-wave (F-W) Cockroft-Walton (CW) and half-wave (H-W) and full-wave (F-W) Dickson, as shown in Fig. 2. The weights of multipliers in each topology achieving different voltage gains are compared and shown in Fig. 3.

At the power and voltage level in this application, and with the device considerations described above, Cockroft-Walton topologies yield lower weight than Dickson topologies when

the number of stages exceeds 2; when the required voltage gain is lower than 8, full-wave topologies yields lower total weight (owing to interleaving reducing output capacitance), and so are strongly preferred. The process of the weight comparison is illustrated below.

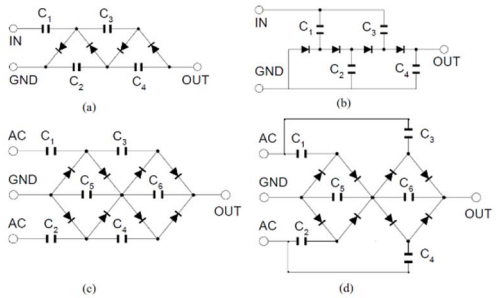

Fig. 2 Typical topologies of voltage multipliers (a). HW CW; b) HW Dickson; c) FW CW; d) FW Dickson.

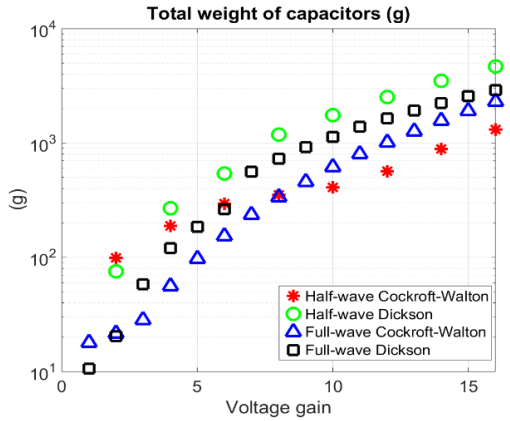

Fig. 3 Total weight of capacitors of Cockroft-Walton and Dickson Voltage Multipliers (20 kV 375 W output)

1) Weight comparison of different topologies

First of all, we pick a topology and the number of stages n, assuming to use this topology to build a voltage multiplier which can satisfy the following three specifications:

a) Output voltage at 20kV and output power at 375W. We only consider half of the desired power and voltage here because one can simply build a bi-polar VM to double the power and voltage.

b) The voltage droop due to the capacitor charge loss is less than 5%. This droop can be calculated using the equation

$$\Delta V_o = \sum_{i=1,2,3,\ldots} \frac{Q_{C_i}}{C_i}$$

Where Q_{C_i} is the charge on capacitor C_i, which can be calculated using the charge vector analysis method in [11].

c) The voltage ripple of the output voltage is less than 5% for all half-wave multipliers. This can be calculated, using the euqation

$$\delta V_o = \sum_{i=1,2,3,\ldots} \frac{Q_{C_{2i}}}{C_{2i}}$$

To simplify the comparison, two assumptions are made: (1) In a given topology, all flying capacitors are the same and all output capacitors are the same. For example, in HW CW VM, C1 = C3, C2 = C4; (2) Output capacitors of FM VM are chosen to be ½ of the flying capacitors since ideally the ripple of two HW would cancel each other.

Then, we decide the capacitance and the number of capacitors based on the above three specifications and Appendix 2.

2) Finalizing the High-Voltage Diode

Cree's C4D02120A, GeneSiC's GAP3SLT33-214 and VMI's VMI150FF3 are used to build three single-stage FW CW VMs in LTspice and compared. To achieve a 20kV output, with Cree or GeneSiC, one either needs to series-connect several diodes in each stage, or needs as many as 20 stages. The latter choice is ruled out due to the added weight of capacitors. The simulation results are shown in Fig. 4.

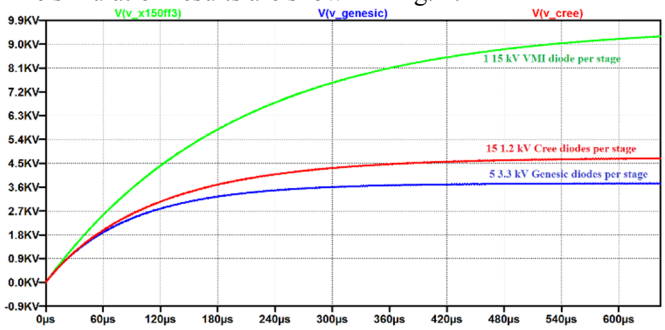

Fig. 4 Output voltages of three single-stage full-wave cockroaft-walton multipliers using three different diodes

The voltage droop with VMI150FF3 diodes is the smallest due to the lower parasitic capacitance. Using multiple SiC diodes theoretically reduces the overall parasitic capacitance, but it still shows unacceptably droop in the simulation. In addition, series-connecting multiple SiC diodes can potentially require balance circuits and add more complexity. Therefore, this option is not further studied in this paper. The VMI150FF3 is selected as the most effective available diode. The design frequency is chosen to be 500 kHz considering the recovery time of 30 ns of the diode.

C. Comparison of isolation stages

Core-based transformers have dominated the isolation stage design in traditional high-voltage converters. The specific power of the transformer improves as the power increases, thus it is especially appealing in high voltage and high power designs.

Tesla-coil and piezoelectric transformers can eliminate the use of a heavy core. However the Tesla coil (constructed without a core) is a highly tuned structure and could potentially be light but may be relatively large because it is coreless [16] [17]. These aspects suggest that it has potential as an approach, but might represent higher risk for an application where both size and weight are important considerations.

Piezoelectric transformers (PZT) can achieve a power density of 40 W/cm3 [18], ideally a specific power of 5 kW/kg, which is higher compared with cored transformers especially at high voltage low power (e.g., tens of watts). They have been used in space applications below 20 kV and 200 W [18 - 21]. However when scaling up in power, one needs to series and

This material is based upon work supported by the Assistant Secretary of Defense for Research and Engineering under Air Force Contract No. FA8721-05-C-0002 and/or FA8702-15-D-0001.

parallel existing PZTs and the advantage on power density are gradually exceeded by the cored transformer as power levels rise.

To illustrate these tradeoffs, isolation stages are designed using these methods and the resulting weights are compared, as shown in Table 1. Cored transformer and Tesla coil are both designed to step up an input voltage of 500V 500 kHz AC to an output voltage of 10 kV, delivering 1 kW. The cored transformer uses ETD49 core, 1:20 turns ratio and PTFE film as the insulation material, resulting in a total weight of 320 g; the Tesla coil is designed following instructions [16] [17]. The PZT-based transformers are designed for the same voltage and power level using existing product from Transonor [20] and STEMiNC [21].

Table 1 Weight comparison of different isolation stages

	Rated power (kW)	Rated voltage (kV)	Total weight (g)	Specific power (kW/kg)
Cored xfmer	1	10	320	3.125
Tesla Coil	1	10	136	7.35
PZT	Use Transonor 100 W 3 kV piece, 3S3P to get 1 kW 10 kV		160x9*	0.695
	Use STEMiNC SMMTF55P6S50 6W 2.5 kV piece, 4S42P to get 1kW 10kV		8x168*	0.74

*The weight are estimated with PZT material of 7.5 g/cm3

The Tesla coil shows doubled specific power, however it only gives an efficiency of 80% thus requires a 250 W increase in the input power from the battery packs. This would result in a max of 200 gram increase in the battery weight, making the advantage of coreless less obvious. In addition, core-based transformers provide more robustness in construction, and more flexible in their use than Tesla coils (as they do not require narrow-band operation), so are preferred.

For the EAD application, a preferred solution of a lightweight high voltage converter is an inverter, coupling to a core-based transformer and a multi-stage voltage multiplier. To simply, we only consider the transformer to have one sectionized secondary. The combination of multi-secondary transformers and multi-stage voltage multipliers could result in more optimal cases, but are not considered in this paper.

D. Resonant Topology Selection

High voltage transformers generally have a large number of secondary turns, resulting in large parasitic capacitances. To incorporate this capacitance, parallel resonant inverter and series-parallel resonant inverter are preferred. A full-bridge series-parallel resonant inverter is chosen because the following three reasons: it provides a factor of 2 in the voltage gain with negligible weight gain; it shows high efficiency in both light load and heavy load; it has a series capacitor to block dc voltage and thus prevent saturation of the transformer [22] [23].

Based on the constraints above, a converter comprising a series-parallel resonant inverter, a ferrite-cored transformer and a 6-stage interleaved full-wave Cockroft-Walton multiplier operating at around 500 kHz yields low weight and good efficiency, as shown in Fig. 5.

III. Design Optimization

A. Optimizing two stages comprehensively

There are several factors influencing the total weight of the inverter and the transformer stage: voltage gains of two stages (thus the values of resonant capacitors and inductor as well as the turns ratio), the winding structure of the high voltage transformer (thus the number of sections, the number of layers, etc). The design space of these two stages is explored comprehensively to minimize the total weight of the inverter, inductor and transformer while maintaining good efficiency.

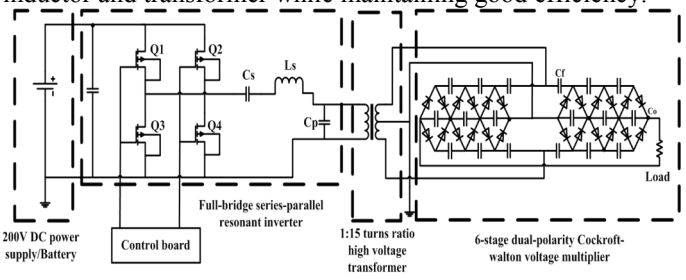

Fig. 5 Topology of a 40 kV 750 W dc-dc converter

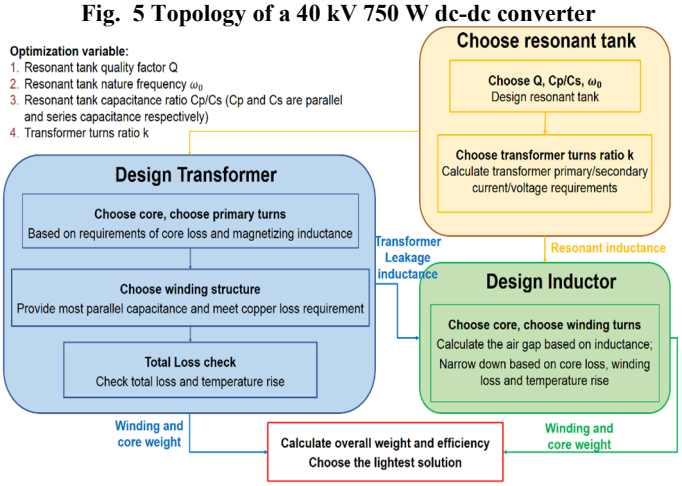

Fig. 6 Optimization flow chart

The optimization process contains three steps, as shown in Fig. 6. In the first step, four variables are swept to determine a resonant tank: the quality factor Q, the natural frequency ω_0, the series and parallel resonant capacitance ratio Cp/Cs, and the transformer turns ratio k; secondly, based on the electrical requirements and k, the transformer is designed; lastly, an external inductor is designed to fill the gap between the transformer leakage inductance and the resonant inductance.

To insure good coupling, both transformer windings are designed to be on the same leg. This yields smaller leakage but increases the efficiency. For each iteration, a transformer and an inductor are designed and the weights are summed together. The weight of each iteration are compared to find the smallest.

B. Transformer Winding Structure Design

When designing the transformer, an important criterion is to use the transformer parasitic capacitance as part of the parallel resonant capacitance.

The parasitic capacitance is dominated by the turn-to-turn and layer-to-layer capacitance of the secondary windings. It increases with the number of turns per layer and the number of

layers [28]. Multi-section secondary is a common solution to reduce the parasitic capacitance. A rule of thumb is that with n-sections the parasitic capacitance can be reduced to 1/n [29]. Different combinations of layer number and section numbers are swept to decide the transformer winding structure.

C. Optimal weight of the inverter and transformer stages

The total weight is mainly contributed by the transformer core, the external inductor and the secondary winding. Stepping from one core to another due to limited window factor or excessive loss normally result in a big step in weight. PQ40/40 core and ETD49 core are the lightest ones that fit our design. ETD49 core in 3F35 is chosen because of its availability, but ideally PR40/40 in either N49 or 3F35 would yield to a ~27 g reduction in weight without sacrificing the efficiency.

With the same transformer core and transformer core loss limitation, different turns ratio yields to different overall weight. When the turns ratio increases, the inductor weight decreases (since less voltage gain is required from the resonant tank) whereas the secondary winding weight increases (since more secondary turns). For ETD 49 core, the optimal point is around a turns ratio of 15 (with 150 secondary windings).

In this case, the required parallel capacitance is around 5 nF. After deducting the stray capacitances and the parasitic capacitance of the diodes, around 1.5nF is need from the transformer. This can be achieved by sectioning the secondary winding into 2. No higher number of sections is needed. Intuitively, higher section number will yield a lower capacitance and may require a bigger inductor thus bigger weight gain. The final component values in the converter are shown in Table 2.

Table 2 Components in the prototype converter

Components		Parts	Value
MOSFETS (Q_1,.., Q_4)		GS66504B	-
Series capacitor C_s		TDK C3216C0G series	19.6 nF
Parallel capacitor C_p		Parasitic capacitances	~ 5nF
Inductor L_s	Core size	RM 14I	33.2 uH
	Material	TDK N49	
	Winding	MWS AWG 14(150/36)	
Trans-former	Core size	ETD49	10:150
	Material	Ferroxcube 3F35	
	Primary	MWS AWG 14 (150/36)	
	Secondary	Teledyne Reynolds 18kV FEP wire	
	Bobbin	ABS material	
Voltage multiplier	C_f/C_o	Murata DHR series	1 nF
	Diodes	VMI X150FF3	-

IV. Experimental Setup and Results

A prototype converter with closed-loop voltage feedback control based on the optimized design was built, as shown in Fig. 7(a). All the sensing, control and driver circuits are integrated on the printed circuit board and it needs no additional components other than a logic power (supplied by a 3.7V LiPo battery) in the EAD application. Fig. 7(b) shows the waveforms of the converter running at 500 kHz and converting 177 V to 38 kV at 500 W. Due to the limitations on the testing load, the converter is tested at three power levels. It achieves an efficiency of 85% at 600 W 40 kV output, 84% at 500W 38 kV output and 81% at 300 W 40 kV output. The weight and voltage gain distribution of the converter are listed in Table 4.

There are three key considerations in construction of the voltage multiplier and the transformer.

1) Transformer bobbin and insulation

To fully utilize the window area, a customized bobbin with two-section secondary is made with ABS material, as shown in Fig. 8. The bobbin is center-tabbed so that the center node can be grounded to insure the symmetry. To increase the electrical insulation, PTFE tape, Kapton tape and high voltage dope are used on the bobbins and windings.

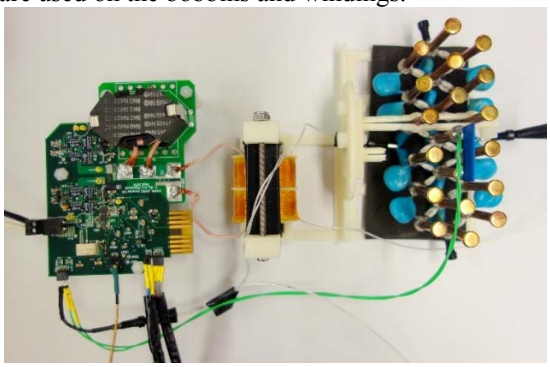

(a)

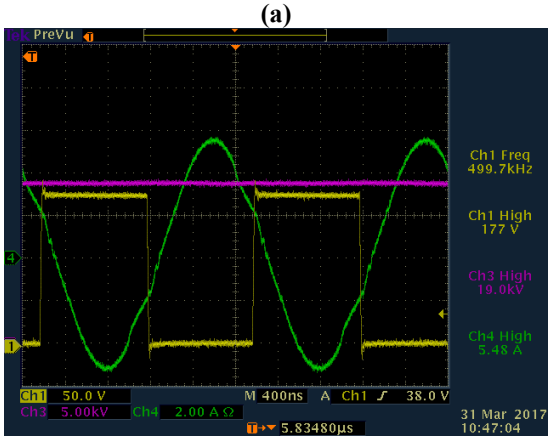

(b)

Fig. 7 40 kV power converter prototype and experimental waveforms at 500 W (Ch1: half-bridge switching node voltage; Ch3: half of the output voltage; Ch4: resonant tank current)

Table 3 Weight and voltage gain distribution of the converter

	Voltage gain	Weight (g)	Weight percentage
Inverter (excluding the inductor)	2.44 – 2.59	56	11%
Inductor		80	15.8%
Transformer	~15	170	33.6%
Rectifier	5.5 – 5.6	110.8	21.9%
Heat sink		89.2	17.6%
Total	201 – 217	506	100%

2) The physical layout of the voltage multiplier

The F-W CW topology is by nature symmetric, thus keeping symmetry in the physical layout is desirable for best operation. Other considerations include 1) keeping the leads of the diode short to minimize the thermal resistance; 2) keeping

each node sufficiently separated from nodes at other potentials to avoid corona discharge; 3) making sure surfaces are sufficiently smooth to avoid corona discharge. We further detail the physical construction of the voltage multiplier and the basis for the key design decisions below.

a) PCB vs non PCB

A non-PCB based voltage multiplier structure is chosen over the PCB-based version for two reasons. First, the PCB adds extra weight despite providing physical support. Second, the PCB adds surface tracking paths. Eventually round bezels in Fig. 9 are used to provide necessary mechanical support to the nodes. It also eliminates the surface tracking paths and provide a smooth, curved surface to reduce the electric field.

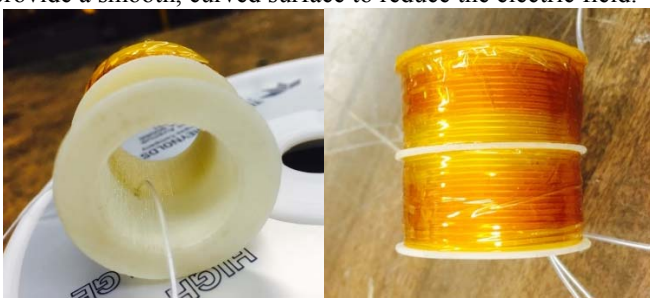

Fig. 8 Customized 2-section transformer bobbins and windings

Fig. 9 Air-insulation (left) and PDMS insulation (right)

Fig. 10 Air-insulation (left) and PDMS insulation (right)

b) Air-isolated vs PDMS-isolated

Potting and oil immersion are two popular methods in building high voltage power supplies to increase both the insulation and heat conduction capabilities; this would be especially valuable for the transformer and voltage multiplier. However, both approaches would add extra mass and more complex manufacture process as compared to an air-insulated design (where one is possible). A PDMS-potted single-stage VM was built and compared with an air-isolated VM, as shown in Fig. 10 (PDMS was chosen instead of Epoxy because its lighter weight and easier manufacture process). At the same input voltage, output voltage and power, the PDMS-potted VM heated up to 74 C, whereas the air-insulated VM heated up to only 50 C. In addition, potting brings much more difficulties for diagnose and reverse engineer; for a full 6-stage VM, the potting material would add ~30 grams of weight.

Thus an air-isolated structure was chosen as it can provide adequate insulation and thermal properties with careful design while yields lighter weight.

3) Heatsink design for the voltage multiplier

Si high voltage diodes are typically used at much lower frequencies (e.g., 200 kHz). Using them at 500 – 700 kHz significantly increases the switching loss thus the temperature. To quantify this tradeoff, a single-stage full-wave CW voltage multiplier was built and tested at various frequencies. The absolute temperature of diodes under tests is shown in Fig. 11. The switching loss significantly increased as the switching frequency exceeded approximately 420 kHz. To process the designed power at 500 kHz and higher, a special heatsink for the diodes was designed. A particular challenge of designing such a heatsink is to keep the electric field low to avoid corona discharge between heatsinks or between heatsink and devices.

Hollow copper tubes or round heat pipes are used for the heatsink, with each tube connecting to one node. Round smooth surfaces of these tubes also help to reduce the local electric field.

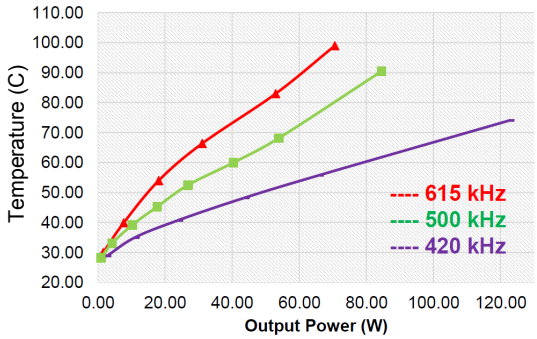

Fig. 11 Temperature of diodes operating at different frequency

The distance between two pipes are set by the length of the diode. One wants to have as short leads as possible to reduce the thermal resistance. Pipes with bigger diameter have better heat transfer capabilities and result in lower local electrical field, at the expense of heavier weight. Longer pipes provide better heat sinking capability.

FEA thermal analysis in Solidworks was conducted for pipes with different length and diameters. It was revealed that with a length of 4 cm, the heat transfer capability of a tube provides the best tradeoff of heat transfer and mass: further increasing the length does not result in justifiable improvement in the reduced temperature. Better heat transfer and lighter weight could be achieved by utilizing heat pipes, but this was not done in the first generation prototype.

FEA electric field analysis was also conducted for pipes with different diameters, as shown in Fig. 12. The strongest electrical field appears on the two ends of the VM, where the voltage is the highest. It needs to be kept below approximately 10 kV/cm, as a conservative rule of thumb to avoid corona. Eventually 3/16 inch copper pipes of 4 cm in length were chosen to be the heatsink.

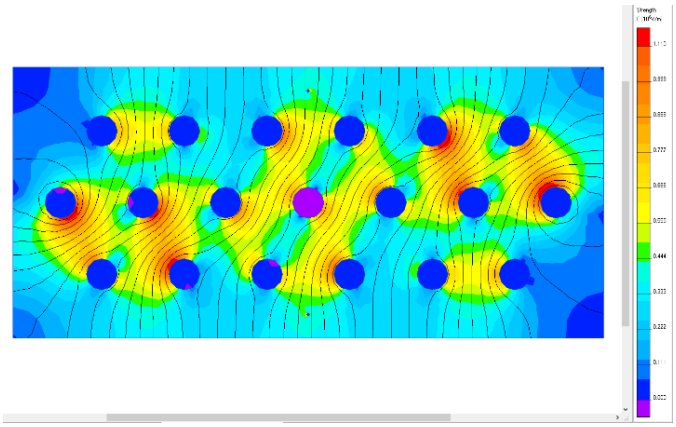

Fig. 12 FEA of the voltage multiplier using 3/16 inch pipe

The prototype converter is used to drive electrode thrusters of an EAD UAV. A 3D printed mechanical mounting structure is designed to fix the voltage multiplier and the transformer. To avoid corona discharge, two inner pipes of the VM are used as the fix point of the structure, where the electric field is the lowest.

The prototype converter is fixed in the nosecone of the UAV, relatively far away from the electrode thruster, which are located near the wings of the UAV, as shown in Fig. 13. The electrode thruster resembles a nonlinear resistive load. At 40 kV, the first-generation thruster design draws about 300 W; at 32 kV, it draws about 150 W. Higher powers may be required in subsequent thrusters. The converter successfully drives both resistor and thruster loads.

V. Conclusion

This paper explores the design space and presents the design of a lightweight high-voltage converter for EAD propulsion applications. Various converter topologies are compared in terms of weight with considerations of device limitations. The weight of the converter is then minimized by design of the voltage gain of each stage. A prototype converter rated at 40 kV and 600 W is built, tested and achieves a specific power of 1.2 kW/kg, far above other designs in its power and voltage class. The approach taken here can likewise be used to facilitate the miniaturization and weight reduction of high voltage converters for many other applications.

Acknowledgment

This material is based upon work supported by the Assistant Secretary of Defense for Research and Engineering under Air Force Contract No. FA8721-05-C-0002 and/or FA8702-15-D-0001. Any opinions, findings, conclusions or recommendations expressed in this material are those of the author(s) and do not necessarily reflect the views of the Assistant Secretary of Defense for Research and Engineering.

Appendix I

Commerical product and research designs compared in Fig. 1 are listed in Table I.

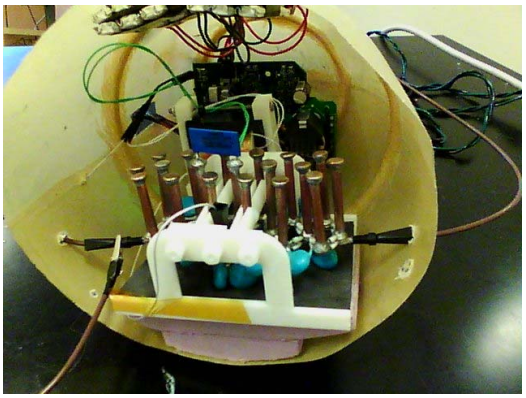

(a)

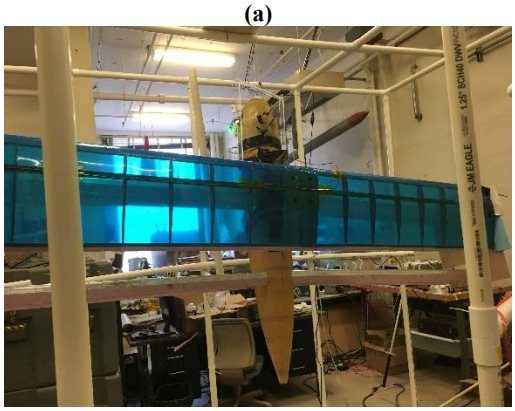

(b)

Fig. 13 The prototype converter in the nosecone (a) and the EAD UAV (b)

Table I High voltage power supplies

Company	Series	Output		Input	Specific weight (kg/kw)
		(kV)	(W)	(V)	
Matsusada	AU	60	1200	100/200 VAC	0.07
	WA	50	1200	100/200 VAC	0.12
	W	40	350	100 VAC	0.09
	W	20	350		0.07
TDK	ALE120A	20	1000	100/200 VAC	0.18
UltraVolt	C series	6	250	30 VDC	0.21
Glassman	EK	60	600	100 VAC	0.07
	EQ	60	1200	100/200 VAC	0.12
HiTek Power	OL1k	60	1000	200 VAC	0.07
Spellman	SLM	70	600	200 VAC	0.09
	SLM		1200		0.1
	SL150kV	150	1200	200 VAC	0.03
EMCO	4000 series	33	10	24 VDC	0.015
Keithley	Model 2290-10	10	100	100/200 VAC	0.027
iseg Spezialelektronik GmbH	HPS 2ND GENERATION	60	3000	230 VAC	6.67
		60	1500	230 VAC	0.075
S. Mao [9]		35	2000	400 VDC	1.75*
D. Fu, et al [10]		10	3700	600 VDC	2.78*
W.C. Hsu [11]		40	300	400 VDC	0.61*
N. Shafiei, et al [12]		10	1100	100 VAC	1.11*

* these are estimated from the paper

Appendix II

A market research of commerical available high voltage capacitors and diodes listed in Table II.

Table II.1 Selected high voltage capacitors

Manufacture	Part No.	Material	Mounting	Rated Voltage (kV)	Capacitance (pF)	Weight (g)	Energy Stored per gram (mJ/g)
Vishay	VJ1206A221JXGAT5Z	Ceramic	SMT	1	220	0.03	3.67
Vishay	VJ1210A222JXRAT5Z	Ceramic	SMT	1.5	2200	0.07	35.36
Murata	DEBE33D102ZA2B	Ceramic	Leads	2	1000	0.32	6.25
Murata	GR455DR73D103KW01L	Ceramic	SMT	2	10000	0.29	68.96
Murata	DECB33J221KC4B	Ceramic	Leads	6.3	220	0.85	5.14
Murata	DECB33J102KC4B	Ceramic	Leads	6.3	1000	2.22	8.94
Vishay	615R100GAST50	Ceramic	Leads	10	500	2.89	8.65
Murata	DHR4E4A151K2BB	Ceramic	Leads	10	150	0.873	8.59
Murata	DHR4E4A221K2BB	Ceramic	Leads	10	220	0.92	11.96
Murata	DHR4E4A102K2BB	Ceramic	Leads	10	1000	2.86	17.48
Murata	FD-10AU	Ceramic	Screw	10	250	16.89	0.74
Murata	DHR4E4B221K2BB	Ceramic	Leads	12	220	1.156	13.70
Murata	DHR4E4B331K2BB	Ceramic	Leads	12	330	1.5	15.84
Murata	DHR4E4B102K2BB	Ceramic	Leads	12	1000	3.52	20.45
Vishay	615R150GATD10AM	Ceramic	Leads	15	1000	18.48	6.09
Murata	DHR4E4C221K2BB	Ceramic	Leads	15	220	1.5	16.50
Murata	DHR4E4C471K2BB	Ceramic	Leads	15	470	2.82	18.75
Murata	DHR4E4C681K2BB	Ceramic	Leads	15	680	3.82	20.03
Murata	DHR4E4C102K2FB	Ceramic	Leads	15	1000	5.6	20.09
Murata	DHS4E4D881MHXB	Ceramic	Screw	20	880	39.3	4.48
Murata	UHV-224A	Ceramic	Screw	20	1000	50.64	3.95
KEMET	746F110GY00M	Film	Leads	2	1100	0.69	3.19
MWS	152MWS402KG	Film	Leads	4	15000	3.289	36.49
MWS	152MWS103KT	Film	Leads	10	15000	8.8	85.23

*Energy stored per gram is calculated by 0.5 x C x (Rated Voltage)^2/weight.

Table II.2 Selected high voltage diodes

Manufacturer	Part No.	Vbr (kV)	Vfr (V)	Cj0 (pF) @ 50V	Recovery		Weight (g)
					Trr (ns)	Qrr/Qc (nC)	
Cree	C4D02120A	1.2	1.8	35	-	11	
	C3D10170H	1.7	2	150	-	96	
Rohm	SCS205KG	1.2	1.6	55	-	17	
Infineon	IDH02SG120	1.2	1.8	25	-	7.2	
VISHAY	BYG2T-M3	1.3	1.39	5 (@20V)	75		0.64
	SF1200/1600	1.2/1.6	3.4	5	75		0.469
GeneSiC	GB01SLT12-252	1.2	1.8	20	-	13	
	GAP3SLT33-214	3.3	1.7	14	-	52	
	GAP05SLT80-220	8	4.6	12	-	8	
Dean technology	SP8SG	8	18	0.8	75		
	UX-F15B	15	16	3.7	50		
Voltage Multipliers	1N6533/SMF6533	5	9	1	70		
	Z100FF3	10	25	8.5	30		
	X100FF3	10	25	2	30		0.5
	X150FF3	15	37.5	2	30		0.51

REFERENCES

[1] Gilmore, CK., Barrett, SRH. "Electrohydrodynamic thrust density using positive corona-induced ionic winds for in-atmosphere propulsion." *Proc. R. Soc. A,* vol. 471. No. 2175. The Royal Society, 2015.

[2] Masuyama K, Barrett SRH. "On the performance of electrohydrodynamic propulsion." Proc. R. Soc. A. Vol. 469. No. 2154. The Royal Society, 2013.

[3] Schwarze, Gene "Development of high frequency low weight power magnetics for aerospace power systems." NASA Technical Memorandum 83656 (1984).

[4] Gilmour, A. S. "High-power, light-weight power conditioning." IEEE Aerospace and Electronic Systems Magazine 6.12 (1991): 33-39.

[5] Myers, I., B. D. Baumann, and R. Kraus. Multi-megawatt inverter/converter technology for space power applications. National Aeronautics And Space Administration Cleverland OH Lewis Research Center, 1992

[6] Gilmour, A. S. "High-power, light-weight power conditioning." *IEEE Aerospace and Electronic Systems Magazine* (1991)

[7] D. Fu, F. C. Lee, Y. Qiu and F. Wang, "A Novel High-Power-Density Three-Level LCC Resonant Converter With Constant-Power-Factor-Control for Charging Applications," *IEEE Transactions on Power Electronics*, Sept. 2008.

[8] J. A. Martin-Ramos, A. M. Pernia, J. Diaz, F. Nuno and J. A. Martinez, "Power Supply for a High-Voltage Application," *IEEE Transactions on Power Electronics*, July 2008.

[9] N. Shafiei, M. Pahlevaninezhad, H. Farzanehfard, A. Bakhshai and P. Jain, "Analysis of a Fifth-Order Resonant Converter for High-Voltage DC Power Supplies," *IEEE Transactions on Power Electronics*, Jan. 2013.

[10] S. Mao, "A high frequency high voltage power supply," Power Electronics and Applications (EPE 2011), *Proceedings of the 2011-14th European Conference*, Birmingham, 2011.

[11] W. C. Hsu, J. F. Chen, Y. P. Hsieh and Y. M. Wu, "Design and Steady-State Analysis of Parallel Resonant DC–DC Converter for High-Voltage Power Generator," in *IEEE Transactions on Power Electronics*, Feb. 2017.

[12] Gu, W-J., and Rui Liu. "A study of volume and weight vs. frequency for high-frequency transformers." Power Electronics Specialists Conference, 1993. PESC'93 Record., 24th Annual IEEE (1993)

[13] Fothergill, John C., Philip W. Devine, and Paul W. Lefley. "A novel prototype design for a transformer for high voltage, high frequency, high power use." *IEEE Transactions on Power Delivery* 16.1 (2001): 89-98.

[14] C. Wu, F. Lee and R. Davis, "Minimum weight EI core and pot core inductor and transformer designs." *IEEE Transactions on Magnetics*, Sep 1980

[15] Raymond, Luke, et al. "27.12 Mhz isolated high voltage gain multi-level resonant dc-dc converter." Energy Conversion Congress and Exposition (ECCE), 2015.

[16] S. Soleyman, Solid State Tesla Coils and Their Uses, http://www.eecs.berkeley.edu/Pubs/TechRpts/2012/EECS-2012-265.html

[17] Tesla coil calculation tool JavaTC http://www.classictesla.com/java/javatc/javatc.html

[18] A.V., Carazo, "50 Years of Piezoelectric Transformers. Trends In The Technology", Material Research Society Vol. 785, 2011

[19] Horsley, E. L., M. P. Foster, and D. A. Stone. "State-of-the-art piezoelectric transformer technology." Power Electronics and Applications, 2007 European Conference on. IEEE, 2007.

[20] Transoner laminated PT, http://www.transoner.com/performance-faq/

[21] STEMINC SMMTF55P6S50 PZT, https://www.steminc.com/PZT/en/ multi-layer-piezo-transformer-55-khz-6w

[22] R. L. Steigerwald, "A comparison of half-bridge resonant converter topologies," *IEEE Transactions on Power Electronics*, Apr 1988.

[23] V. Garcia, M. Rico, J. Sebastian and M. M. Hernando, "Using the hybrid series-parallel resonant converter with capacitive output filter and with PWM phase-shifted control for high-voltage applications," *IECON '94.*

[24] L. Dalessandro, F. da Silveira Cavalcante and J. W. Kolar, "Self-Capacitance of High-Voltage Transformers," in *IEEE Transactions on Power Electronics*, vol. 22, no. 5, pp. 2081-2092, Sept. 2007